Budownictwo i Architektura 24(3) 2025, 145-170

DOI: 10.35784/bud-arch.7900
Received: 11.06.2025; Revised: 29.08.2025;
Accepted: 04.09.2025; Available online: 15.12.2025

Orginal Article

Analytical modeling of the dynamic thermal behavior of stabilized compacted earth blocks walls for bioclimatic constructions

M'hamed Mahdad[1], Aghiles Hammas[2,*], Said Abboudi[3]

[1] Centre National d'Etudes et de Recherches Intégrées du Bâtiment; Souidania-Algiers. 16097, Algeria;
mahdadcnerib@gmail.com; ORCID: 0000-0002-6957-0648
[2] Centre National d'Etudes et de Recherches Intégrées du Bâtiment; Souidania-Algiers. 16097, Algeria;
a.hammas@cnerib.edu.dz; ORCID: 0000-0003-3107-2480
[3] Université Marie et Louis Pasteur; UTBM; CNRS; Laboratoire Interdisciplinaire Carnot de Bourgogne; ICB UMR 6303, Belfort Cedex, F-90010, France
saidabboudi@utbm.fr; ORCID: 0000-0001-7420-1014
[*] corresponding author

Abstract: The main challenge in bioclimatic constructions using compressed and stabilized earth blocks (CSEB) is determining the optimal external wall thickness to ensure good thermal comfort. This study investigates heat transfer through opaque walls made with various CSEB samples commonly used in Algeria, using the cyclic admittance method. Five homogeneous CSEB materials were evaluated based on several dynamic thermal parameters: admittance (Y), transmittance (U), surface factor (F), decrement factor (DF), and time lag (TL). Results showed that walls made with CSEB-2 material at 40 cm thickness had the best thermal performance. Additionally, multiple linear regression (MLR) analysis was applied to predict TL and U values, yielding high coefficients of determination (R^2 of 0.98 and 0.79, respectively). The study concluded that TL and U values are strongly influenced by wall thickness and the compaction energy of the CSEB samples.

Keywords: Earth blocks, Bioclimatic constructions, Admittance method, Thermal inertia, Thermal performances, Multiple linear regression analysis

1. Introduction

The use of thermal inertia in the design of wall building envelopes, particularly in regions characterized by arid and dry climates such as southern Algeria, significantly enhances indoor thermal comfort. Over recent decades, the thermal performance of wall structures made from compressed and stabilized earth blocks (CSEB) under such climatic

conditions has not been sufficiently investigated in either analytical or experimental studies [1-4]. Furthermore, due to the lack of research in this area, the design and dimensioning of envelope walls using CSEB materials in Algerian earthen constructions have been only minimally addressed in previous scientific literature.

CSEB materials used in earthen construction are primarily valued for their economic advantages, especially in terms of energy efficiency compared to other conventional building materials. In construction, CSEB is produced by adding a suitable amount of stabilizing agents to compressed earth blocks (CEB), which are formed by compressing soil under specific pressure conditions [5]. The stabilization process can involve various mechanical and chemical methods aimed at enhancing the material's mechanical strength, durability, and stability. The effectiveness of this process largely depends on the type and amount of stabilizer used.

Notably, this type of construction exhibits good thermal performance throughout its service life [6,7]. Thanks to the high thermal mass of CSEB materials, they can absorb more heat when exposed to a heat source compared to other materials [4,8], and they release the stored heat more gradually over time [9]. For this reason, several studies have aimed to improve their performance by proposing different energy-efficient envelope designs [10-12]. However, in the case of CSEB-based earthen construction, wall dimensions are often determined empirically, despite the limited scientific research available in this field [13].

In recent years, analytical studies exploring the role of thermal inertia in heat transfer through building walls and flat roofs have gained significant attention in the construction sector [4,14-16]. As a result, several methods have been developed to estimate the thermal inertia of external walls and flat roofs, including the Exact Method, the Transfer Function Method (TFM), the Cooling Load Temperature Difference Method (CLTD), and the Total Equivalent Temperature Difference Method (TETD) [17-19].

All of these methods are widely applied in the construction sector, particularly for conventional materials such as concrete, terracotta brick, stone, and various types of insulation. Granja et al. [20] proposed a periodic solution for modeling heat flow through flat roofs using Fourier analysis. Similarly, Lu et al. [21] developed a new analytical method based on Fourier series analysis to study one-dimensional transient heat conduction through a composite slab under periodic boundary conditions. This method has proven to be efficient, accurate, and does not require numerical computation.

The admittance analytical method, which is based on complex Fourier analysis, has proven to be highly effective for studying periodic heat transfer through building roofs and walls [22,23]. Compared to other analytical approaches, the admittance method – built upon the transmission matrix offers several advantages, including a matrix format that facilitates data storage and modeling analysis [24]. This method accounts for the effects of dynamic conditions on heat transfer, as well as sorption and thermal storage phenomena within the wall materials [25].

In recent years, several studies have focused on the dynamic thermal characterization of walls using the admittance method [26]. For example, Shaik et al. [22] examined the influence of thermophysical properties and material thickness on the thermal behavior of walls and roofs. In a related study, the same authors investigated the dynamic thermal response of a wall made from laterite rock using this method [27], analyzing the effects of ambient air relative humidity and temperature on unsteady-state heat transfer for various wall thicknesses.

Additionally, Kalinović et al. [28] applied the admittance method to analyze the dynamic thermal response of multilayer walls under periodic external thermal excitation, with the goal of optimizing insulation placement within composite wall systems. Nematchoua et al. [13] explored the optimal thickness of expanded polystyrene insulation for external CSEB walls in the tropical climate of Douala, Cameroon. Their findings highlighted

that optimal wall thickness is strongly influenced by both material properties and local climatic conditions.

El Fgaier et al. [29] investigated the dynamic thermal performance of three types of raw earth walls to determine the appropriate thickness for achieving optimal thermal inertia. Their results indicated that the most effective wall thickness – yielding maximum heat capacity and time lag – ranges between 30 and 40 cm. In a similar context, Niya et al. [30] evaluated the impact of insulation and thermal mass on the envelope of a stabilized earth block test cell under the hot, dry tropical climate of Burkina Faso.

However, in the context of Algeria, the thermal performance of stabilized earth blocks used in bioclimatic construction has been only marginally investigated. To address this gap, the present study aims to conduct an optimization analysis to assess the thermal performance of wall envelopes made from compressed and stabilized earth blocks (CSEB). The primary objective of this research is to apply the analytical admittance method to characterize the dynamic thermal parameters of homogeneous external walls in earthen buildings located in hot and arid regions of Algeria.

The study begins with experimental investigations conducted on a prototype test structure built using CSEB blocks at the CNERIB Research Center in Algiers, northern Algeria. Following this, the proposed analytical model is validated against the thermal performance results obtained from the CSEB walls and is then extended to evaluate other types of CSEB wall configurations. Additionally, multiple linear regression (MLR) analysis is applied to predict various key thermal parameters investigated in the study, including the decrement factor (DF), time lag (TL), transmittance (U), and admittance (Y).

2. Materials and methods

This work focuses on the thermal dimensioning of external walls constructed with CSEB earth blocks, which are widely used in Algerian bioclimatic buildings (Fig. 1). Currently, there is a lack of comprehensive studies that clearly define the optimal configuration of these building envelopes. In response, this study employs an analytical approach to optimize the design of external walls for earthen constructions under Algerian climatic conditions.

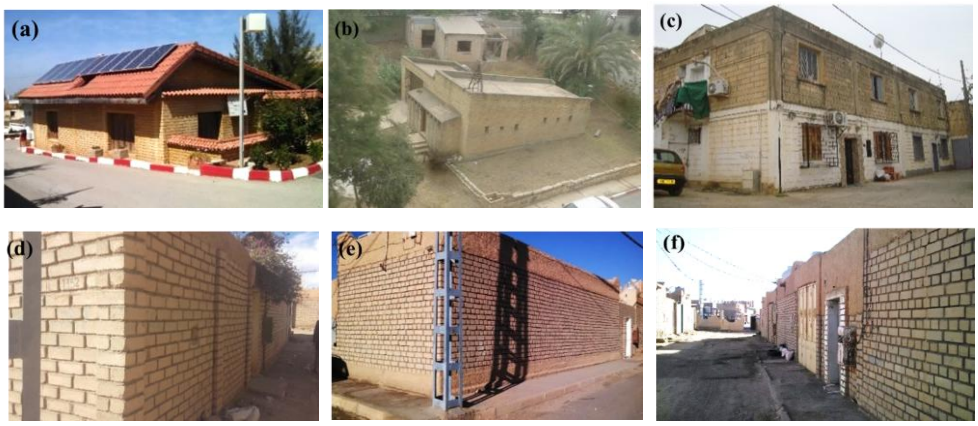

Fig. 1. Load bearing soil-cement blocks residential building in the a) Medenec prototype CNERIB-Algiers, b) Bioclimatic prototype CNERIB-Algiers c) Houses at Cheraga-Algiers, d) Tamanrasset building cities, e) Houses at Adrar, f) Houses at Mouflon – Tamanrasset

In Algeria, climatic conditions vary significantly between the northern and southern regions. In the north, temperature values fluctuate with altitude. The coastal zone is characterized by a Mediterranean climate, with hot, dry summers and mild, rainy winters, receiving an average annual rainfall of approximately 600 mm [31]. Winter temperatures typically range from a minimum of around 9 °C to a maximum of about 17 °C, while summer temperatures range from 30 to 34 °C, with nighttime lows around 21 °C. The annual temperature variation from 2000 to 2016 in the Souidania-Algiers region is presented in Fig. 2. In this area of moderate climate, the typical thickness of external envelope walls is generally around 45 cm.

In contrast, the climate conditions in the Algerian Sahara, such as in the Adrar region, are much more extreme, as described in [6]. In these hot and arid environments, the thickness of CSEB external walls is typically increased to approximately 50 cm to ensure better thermal insulation and improved indoor comfort.

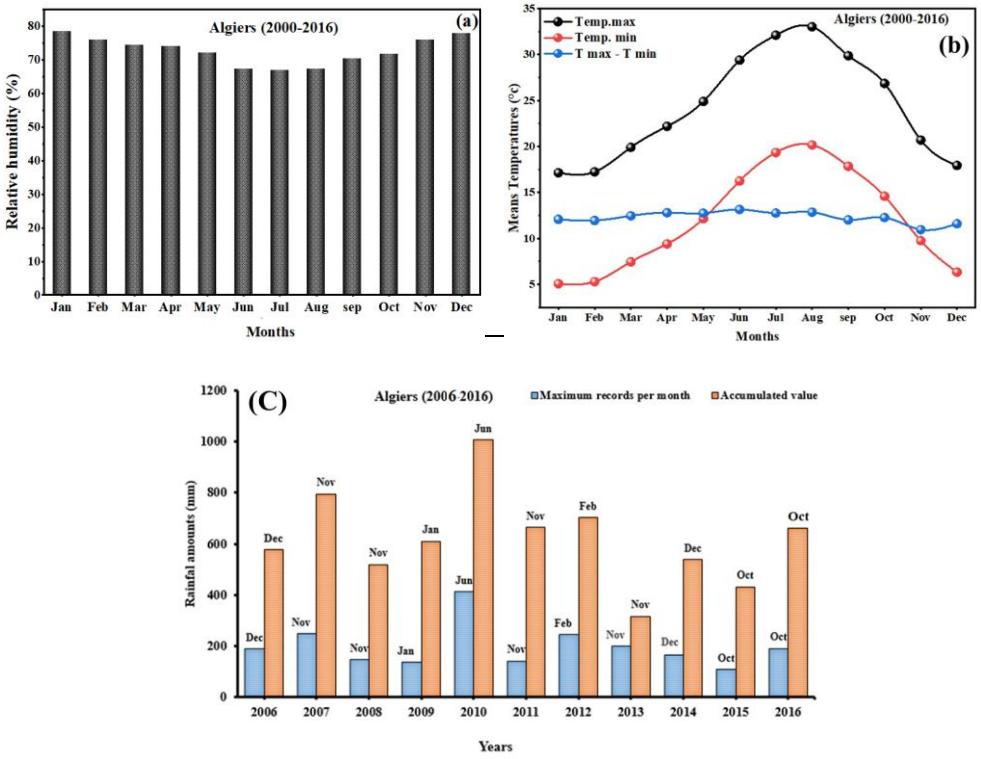

Fig. 2. Evolution of annual temperature from 2006 to 2016 in the Souidania-Algiers city: (a) relative humidity, (b) mean temperatures, and (c) rainfalls [32]

2.1. Building materials and wall systems

This study focuses on optimizing the thickness of external homogeneous walls constructed with CSEB blocks, commonly used in traditional buildings located in the hot and dry climates of northern and southern Algeria. The analytical admittance method was selected to analyse the dynamic thermal parameters of five different types of CSEB walls (see Appendix 1).

The thermo-physical properties of the CSEB samples used for building the homogeneous wall configurations were experimentally measured to provide accurate input data for the analytical model [22,40].

2.2.1. Selection of homogeneous walls

In this study, all CSEB blocks are produced using a semi-automatic hydraulic press machine that applies high compaction energy exceeding 5 MPa (see Fig. 3a). This machine, developed in Algeria with the collaboration of the CNERIB Centre, features a double-shell metal mold equipped with specialized components to ensure consistent block quality [33,35].

The manufacturing process of the CSEB materials is illustrated in Fig. 3b-c. A measured quantity of soil is placed into the mold, which is then subjected to compression to produce a properly compacted block. Then the dosing tray is filled with abundant soil prepared at the Proctor point. To ensure the homogeneity of the blocks, the mold is always filled with a consistent amount of material using a dosing container. Once the mold is filled and leveled, the dosing tray is rotated to evenly distribute the soil within the compaction mold. To reinforce the corners, fingers can be pressed into the four corners of the mold before the soil is fully distributed, resulting in stronger compression at these critical points. It is important to note that compression is applied only after filling the mold with an optimal volume of soil mixture. The resulting earth blocks are parallelepiped in shape with standard dimensions of 29.5 × 14 × 9 cm [33].

Fig. 3. Confection process of CSEB earth blocks. a-Machine of semi-automatic hydraulic press. b-rotate the dosing, c-block compact

In order to investigate the thermal performance of CSEB blocks as envelope material, various homogeneous configurations of typical wall structures have been studied, see Fig. 4.

CSEB wall-1 CSEB wall-2 CSEB wall-3 CSEB wall-4 CSEB wall-5

Fig. 4. Homogeneous configurations of CSEB wall block

All the characteristics of the CSEB earth blocks used in this study were obtained from various research projects conducted at the CNERIB Centre [2,33,34]. These materials result from the stabilization of sandy soil, a locally abundant resource in Algeria [35]. In this work, cement is used as the stabilizer, with varying contents of 6%, 8%, and 10%.

The selection of these five different types of CSEB materials is based on their availability and the manufacturing methods commonly used across Algeria. Indeed, the knowledge of CSEB earthen construction, including the choice of suitable soil and manufacturing techniques, has been traditionally passed down through generations in the country. However, despite this long-standing practice, there is a lack of detailed scientific studies and standardized guidelines for constructing CSEB earth houses that ensure good thermal comfort and optimal external envelope design in Algeria [2,33].

In this study, CSEB-1 is made from the same soil used for the exterior wall construction of the Souidania-Algiers PM prototype (northern Algeria), as shown in Fig. 1a. This location is characterized by a temperate Mediterranean climate (see Fig. 3). CSEB-2, manufactured with the same earth soil, constitutes the exterior wall blocks of a house located in Mouflon, in the town of Adrar (southern Algeria), shown in Fig. 1c. CSEB-3 was prepared using clay-sand soil sourced from the site of Douera (northeast Algiers). CSEB-4 was built using the same earth soil as that used for the exterior wall blocks of the MEDENEC prototype in Souidania-Algiers, as illustrated in Fig. 1b. Finally, CSEB-5 was prepared from clay-sand soil collected from the Cheraga deposit (northern Algiers).

2.2.2. Thermo-physical properties

In this study, the thermal and physical properties of all blocks were measured using the Ct-meter instrument from SMEE [36], which employs the hot wire method (see Fig. 5). This device operates in accordance with the EN 993-15 standard [37]. Additionally, thermal conductivity measurements followed the ASTM C518-21 standard [38], while heat capacity and density were determined according to ISO 12571 [39]. The results obtained from these tests, summarizing the thermophysical properties of the materials, are presented in Table 1.

Fig. 5. Thermal test (Ct-meter)

Table 1. Thermophysical properties of all CSEB blocks

Blocks	cement (%)	Compaction (MPa)	λ (W/mK)	ρs (Kg/m^3)	Cp (J/kgK)
CSEB-1	8% cement	15 MPa	1.10	2000	936
CSEB-2	6% cement	7 MPa	0.75	2100	1054
CSEB-3	6% cement	7 MPa	1.053	2091.2	995
CSEB-4	6% cement	7 MPa	1.139	2013.65	1016.71
CSEB-5	10% cement	10 MPa	0.951	1873.9	1135.9

2.2. Analytical method

In this study, the dynamic thermal properties of the different wall systems were evaluated using the analytical admittance method implemented through a MATLAB program. This method follows the guidelines outlined in the ISO 13786 standard [40]. All dynamic thermal parameters were calculated using the equations provided in Appendix 1.

The calculations were performed for a homogeneous, opaque wall subjected to an external sinusoidal temperature variation with a period P = 24 h and an internal temperature Ti=25°C. The thermo-physical properties of the CSEB blocks were obtained experimentally in the laboratory. The values of the internal Ri and external RO thermal resistances (Ri = 0.045 and RO= 0.11 m^2KW^{-1}) [3]. The effect of humidity parameter on the thermal properties of CSEB materials was not considered in the analysis.

2.3. MLR analysis

The description of the relationship between the dependent (Y) and different considered independent variables (Xi) is generally used by MLR analysis. For this purpose, the suitable model was developed for the prediction of the dependent variable values using this statistical method. The general form of the MLR model is expressed as indicated in the following equation:

$$Y_i = b_0 + \sum_{j=1}^{i} b_j X_j + \varepsilon_i \tag{17}$$

where Y_i translates the values of dependent variable (compressive strength values); X_i $(i = 1,2,\dots,p)$ presents the three studied independent variables of wall thicknesses, cement content and compaction pressures; b_j $(j = 1,2,\dots,i$ indicate the values of the estimated parameters of the model and ε_i is the model random error. According to the previous investigated work about the prediction model using the MLR analysis, there are several specific software that can be used for the development of predictive models by the application of MLR analysis [41]. However, two statistical software are used in this study namely SPSS (Statistical Package for Social Sciences) and Excel.

3. Results and discussions

3.1. Validation of the applied analytical method

For the validation of the applied analytical method, an experimental investigation was conducted at the CNERIB site in Souidania, Algiers. The collected data includes measurements of ambient air temperatures on both sides of the envelope walls of the CSEB construction prototype (see Fig. 6).

The external walls of the prototype were built using CSEB materials prepared from very sandy soil stabilized with 6% cement and compacted with an energy of 7 MPa. The CSEB blocks have dimensions of 29.5 cm in length (l), 14 cm in width (w), and 9 cm in height (h). Specimens extracted from the exterior face of the prototype envelope were utilized in the present validation study. The thermo-physical properties of the wall materials are characterized by a density of 2036 kg/m³, a thermal conductivity of 1.12 W/(m·K), and a specific heat capacity of 1035 J/(kg·K). The prototype was constructed with homogeneous walls composed of CSEB blocks with a total thickness of 40 cm (Fig. 6).

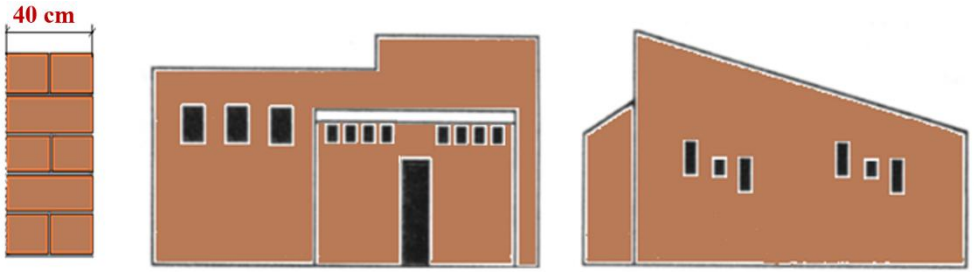

Fig. 6. a) CSEB structure of the investigated external wall, b) General architectural aspects of orientations façades of South-East and c) South-West

Among the series of measurements carried out in the summer month of August in the climatic context of the Algiers region, the days from 25 to 30 August selected served as the basis for the analysis, resulting from the fact that the peaks in surface temperature recorded for the south-facing wall were the highest [2,3,34].The evolution of the temperature parameters on the external and internal faces of the wall of the prototype is showed in Fig. 7.

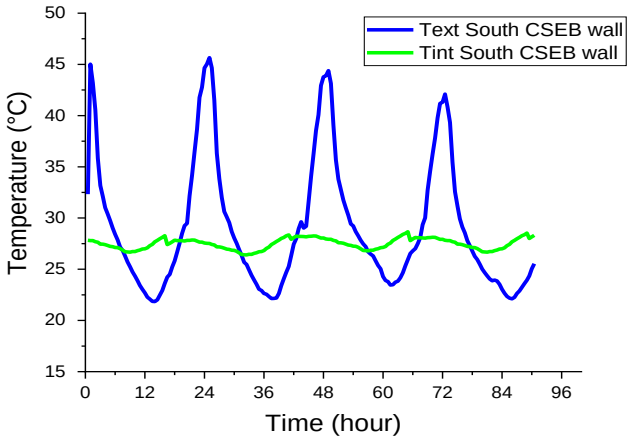

Fig. 7. Experimental time series representing the indoor and outdoor summer temperatures of the south face CSEB wall

Table 2 presents the results of the thermal performance of the south-facing walls of the prototype, corresponding to the hottest day of the summer season in the Algiers region. The table compares the calculated values obtained from the analytical model with the measurements gathered during the experimental investigation.

The comparison of the thermal response of the CSEB walls prototype under climatic conditions of north Algeria (Algiers) made it possible to identify the parameters of the thermal inertia of the wall made with CSEB materials. This concerns in this case the decrement factor and the time lag of the heat wave through the southern external wall.

Indeed, for walls designed with a homogeneous configuration with a thickness of 40 cm, an internal thermal phase with an average of (12.52 hours) is noted and the value of the calculated decrement factor is 0.13.

Table 2. Time lag and decrement thermal values.

Day	TL(exp) (hour)	DF (exp) (-)
1	12.58	0.12
2	12.53	0.13
3	12.50	0.13
4	12.49	0.14

Calculation of the thermal inertia parameters with the admittance method using equations (14) and (15) yielded conclusive results close to those of the experimental investigation, with a time lag of around 12.50 hours and a decrement factor of around 0.136, respectively.

The application of the analytical method will be extended to other configurations of homogeneous earthen walls to optimally determine the thickness of these walls. The analysis of the results will identify the key factors influencing the appropriate dimensioning of the homogeneous envelope walls, aiming to ensure satisfactory thermal comfort in earthen constructions under the hot and arid climatic conditions of Algeria.

3.2. Effects of the wall thickness on TL and DF parameters

The thermal inertia of the building envelope built with CSEB materials may be evaluated through the dynamic factors of time lag (TL) and decrement factor (DF), [4,14]. In the scientific literature, it is well known that the decrement factor should have low values in order to reduce the magnitude of the heat wave across the wall, which is not the case for the time lag, which should have the highest possible values [4,42]. The values of these two parameters are mainly dependent on the external and internal temperatures as well as the thermo-physical properties of the materials that make up the wall layers [25].The effects of homogeneous wall thickness on the decrement factor (DF) and time lag (TL) of CSEB blocks were shown in Fig. 8a-b.

According to the results obtained in this study, it can be seen that the decrement factor values decrease when the thickness of the CSEB wall increases. In contrast, the time lag increases with the increasing thickness of the wall, which is mainly due to the high capacity of the CSEB materials to absorb the heat flow. In addition, the thermal storage capacity of the thick walls is higher than that of the thin walls. It should be noted that this characteristic involves a shift in the temperature distribution of the exterior and interior walls, which increases the time lag significantly. The decrement factor and the time lag factor are calculated by equations (14) and (15).

In contrast, it can be clearly seen that the time lag values increase and the decrement factor decrease in the walls built with a CSEB with a lower thermal conductivity (case of W2 and W5 blocks). These two walls were built with blocks characterized by thermal conductivities of 0.75 and 0.95 W/mK, respectively. The other walls are built with CSEB blocks with a few high thermal conductivities, which allows heat flux to be easily transferred through these walls (W1 and W4). In addition, the decrease in decrement factors and the increase in time lag are mainly due to the increasing specific heat capacity of blocks. Indeed, the increase in the specific heat capacity of the materials leads to an increase in the thermal performance of the wall. Similarly, increasing thermal mass (characterized by the density, specific heat and wall thickness) can effectively increase time lag (TL) and decrease decrement factor (DF) values. This result is obtained for all walls of the study (W1 to W5).

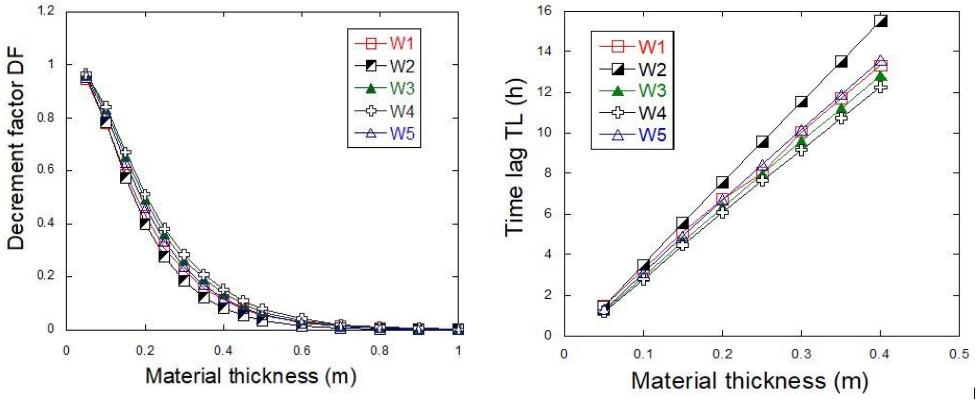

a) b)

Fig. 8. Effect of walls thickness on the (a) heat flux time lag and (b) decrement factor

The specific heat capacity and the thermal conductivity are very important characteristics to evaluate the heat storage capacities and the efficient energy of the CSEB walls [4]. Similar conclusions are obtained for the relationship between the thermo-physical properties and the parameters of the thermal inertia of CSEB earth walls have also been noted by other researchers [14].

Walls with lower decrement factors and higher time lags have a greater capacity to reduce temperature fluctuations, thereby ensuring better thermal comfort inside buildings. Among the five CSEB walls studied, at a thickness of 40 cm, the W2 wall exhibits the lowest decrement factor (0.081) and the highest time lag (15.49 hours). This performance is attributed to its higher sand content and compaction level, which increase density and enhance thermal inertia, effectively delaying heat transfer. In contrast, the W1 wall, made from CSEB-1 blocks, shows the highest decrement factor (0.168) and the lowest time lag (11.82 hours). These results are mainly due to the decrement factor and time lag associated with the intrinsic thermo-physical properties of the materials, including conductivity and specific heat.

Thus, the configuration with (CSEB 2) wall block increases the time lag (TL) by 1.31 compared with the configuration of (CSEB 1). Consequently, the decrement factor (DF) value was reduced by around 1.08 compared to (CSEB 1) wall. Similarly, the configuration with CSEB3 blocks increases the time lag (TL) by 1.45 compared to (CSEB 1) wall. While the value of the decrement factor (DF) is reduced by about 80% compared to the (CSEB 1) wall. On the other hand, for the walls built with a CSEB-1, CSEB-3 and CSEB-4 blocks, the optimal thickness that gives a good thermal comfort is in the range of 35 and 40 cm, with time lag equal to 10.33-11.82, 10.71-12.25, 10.55-12.03 hours, respectively.

3.3. Effect of wall thickness on thermal admittance and thermal transmittance

The thermal performance of the homogeneous walls was also assessed by analyzing the variation of thermal admittance and thermal transmittance as functions of wall thickness. Thermal admittance represents the rate at which heat is conducted through one side of the wall in response to temperature fluctuations on that same side [22,27]. Figures 9a-b illustrate how thermal transmittance and thermal admittance values change with varying wall thicknesses.

The periodic thermal transmittance (Y) generally translates the opposite capacity of an opaque wall to stop a heat flu which crosses over 24 h [24]. The results of this analysis show that all walls made from CSEB materials exhibit a similar trend in terms of dynamic thermal behavior. Nevertheless, there was a clear difference between the evolution of the two parameters in the case of thermal admittance and thermal transmission, as well as the wall thickness increases lead to the decrease significantly of the transmittance values, (Fig. 9a). Indeed, this observation is applied for all the five CSEB walls thicknesses. The results indicate that for thermal dynamic properties such as thermal admittance (Y), this parameter increases with wall thickness up to approximately 20 cm. Beyond this thickness, the Y values stabilize across the studied wall configurations. Conversely, thermal transmittance (U) is mainly influenced by both wall thickness and the total thermal resistance, as illustrated in Fig. 9b. Indeed, the U values should be lower as possible in order to reduce the building cooling load and energy gain as reported in literature [14,28].

The W2 configuration, based on CSEB-2, exhibits the lowest thermal transmittance values across all wall thicknesses among the five CSEB materials studied, followed by the W5 homogeneous wall based on CSEB-5. These wall configurations demonstrate superior thermal performance in terms of energy storage and heat flow reduction, representing the most efficient earth material options among those analyzed. Hence, in the range of thickness of 30 and 40 cm, the dynamic property of the admittance for W3 configuration wall is around 4.88 $W \cdot m^{-2} \cdot K^{-1}$. This parameter is generally correlated to the density, thermal capacity, thermal conductivity and wall thickness.

In this study, the thermal transmittance values for walls thicknesses in the range 30 to 40 cm is obtained between 1.75 and 1.42 $W \cdot m^{-2} \cdot K^{-1}$. These low values are mainly attributed to the low of the thermal conductivity and specific heat capacity of blocks, 0.75 $W \cdot m^{-2} \cdot K^{-1}$ and 1054 $J \cdot kg^{-1} \cdot K^{-1}$, respectively. In addition, in the same range thickness, the admittance and thermal transmittance values of W5 is 5.07 $Wm^{-2} \cdot K^{-1}$ and from 2.05 to 1.69 5.07 $W \cdot m^{-2} \cdot K^{-1}$, respectively. In the other hand, it can be clearly seen from Figure. 9 that the homogeneous walls W4 (CSEB-4) gave the highest thermal transmittance values with a low thermal performance for the different thicknesses of the walls in the range of 50 to 100 cm.

Similarly, for a wall thickness between 30 to 40 cm, the calculated admittance and thermal transmittance values for W4 is around 5.22 $W \cdot m^{-2} \cdot K^{-1}$ and 2.30 to 1.89 $W \cdot m^{-2} \cdot K^{-1}$, respectively. Compared to the other walls of W2 and W5, it can be observed a significant difference due to the low thermal resistance of the block CSEB-4 so that the heat flux is easily transferred through these walls. Hall et al. reached similar conclusions in their study on the thermal performance of earth walls using the admittance method [43]. Specifically, for homogeneous rammed earth walls stabilized with 6% cement and a thickness of 40 cm, they reported thermal admittance values ranging from 4.7 to 5.7 $W \cdot m^{-2} \cdot K^{-1}$, with thermal transmittance varying between 1.26 and 2.30 $W \cdot m^{-2} \cdot K^{-1}$.

In addition, these two parameters (Y and U) are primarily influenced by variations in wall humidity. Indeed, a non-uniform linear distribution of moisture within the solid wall leads to a significant increase in thermal transmittance. Shaik et al. concluded that for each wall thickness, the thermal parameters (Y and U) increase linearly with thickness up to a constant value around 20 cm [22]. Similar findings were reported by Balaji et al. [44], who observed comparable trends in thermal admittance and transmittance for varying envelope thicknesses of homogeneous CSEB materials. Notably, at lower wall thicknesses, the values of admittance and transmittance are nearly equal and highly dependent on wall thickness.

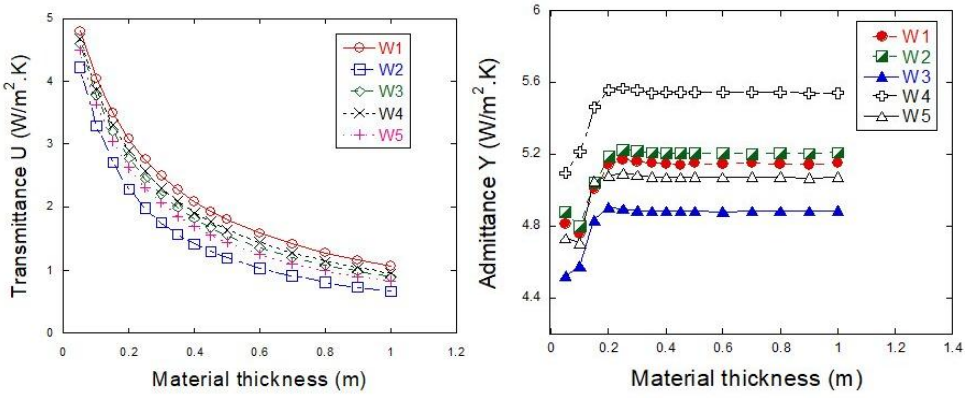

a) b)

Fig. 9. The effect of walls thickness on thermal (a) transmittance and (b) admittance

3.4. The surface factor as a function of the thermo-physical properties

Figure 10 indicates the surface factor progression as a function of the thickness of homogeneous walls based CSEB materials.

As clearly seen from these results indicated in this figure, the evolution of the surface factor as a function of the thickness of the walls follows almost the same tendencies, for all homogeneous configurations. In addition, there is stability in the evolution of the surface factor values beyond a wall thickness limit (between 15 and 20 cm). The values obtained for W2 and W5 walls, which have better thermal performance, are equal to 0.36 and 0.34 respectively, while the results obtained for W3 walls is 0.32. Indeed, the relationship between the surface factor and thickness walls can be separated into two sections. In the first, the surface factor increases with increasing of walls thickness, while in the second part, a stabilization phase of the values has been indicated. However, for W2 and W5 with high thermal performance, the surface factor obtained is equal to 0.36 and 0.34, respectively. In the case of walls with low thermal performance, the F-value of the (W1, W3, W4) walls made is almost identical (0.31 and 0.32, respectively). According to these results, it can be noted that CSEB construction materials with high thermal conductivity have lower surface factors and high time lag. The surface factor should be as low as possible, while the time lag should be as high as possible to ensure a slow response of the wall to short-wave radiation [8,14,28]. The behavior of the surface factor parameter is strongly influenced by the thermal properties and thickness of the layer directly exposed to the heat flux. Shaik et al. [22] indicates more details about the effect of humidity on the surface factor walls. Indeed, they observed on the one hand, the surface factor of laterite rock walls decreases with the increase of the humidity content at the ambient air. On the other hand, the time lag of the surface factor increases with the rise in the relative humidity of the ambient air due to the increase in the thermal conductivity of the laterite rocks with the relative humidity [14-45].

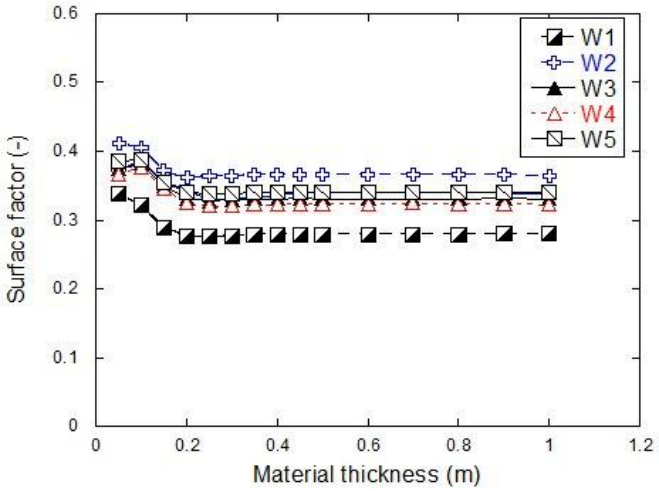

Fig. 10. Variation effect of thickness walls on the surface factor

Figure 11 illustrates the variation of the surface factor in relation to the thermal conductivity of the CSEB blocks. For the homogeneous walls studied, the results reveal an inverse relationship between the surface factor and thermal conductivity, meaning that as thermal conductivity increases, the surface factor decreases.

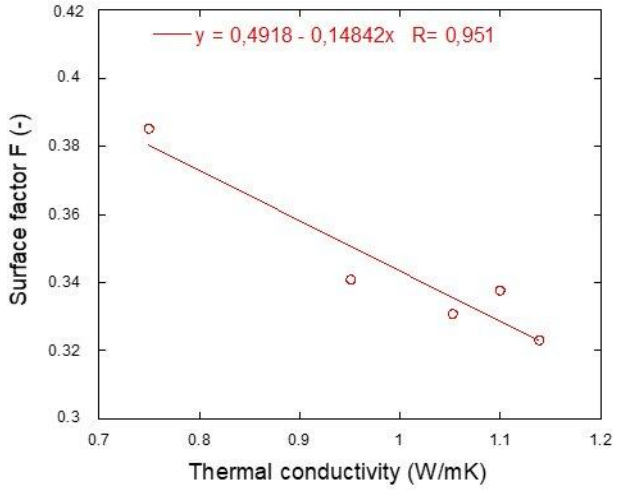

Fig. 11. Effect of the thermal conductivity on the surface factor

3.5. Design optimization CSEB wall considering thermal mass

Previous studies have found that at an optimal wall thickness, heat flux takes approximately 10 to 12 hours to pass through the building envelope, resulting in acceptable thermal comfort [4,30,46-48]. In this study, for a wall thickness of 40 cm, the earth block material CSEB-2 demonstrated superior thermal performance, with the lowest decrement factor (0.081) and the highest time lag (15.49 hours) among the five materials analyzed.

These findings align with conclusions drawn by El Fgaier et al. [29] and [40]. For the W2 wall, a decrement factor of 0.40 and a time lag of 7.58 hours were observed at a thickness of 20 cm. Indeed, the W3 wall with a thickness of 30 cm appears to provide good thermal comfort, with a low decrement factor of 0.18 and a high time lag of 11.53 hours.

In addition, the decrement factor values for the walls W4 and W5 at the same thickness of 30 cm are 0.22 and 0.23, respectively. The time lag obtained for these two walls is 10.04 and 10.14 hours. Consequently, the optimal thickness that gives a good thermal comfort is in the range of 35 and 40 cm, with time lag equal to 10.33-11.82, 10.71-12.25, 10.71-12.25 hours, respectively. Accordingly, it can be noted that these results appeared to be in good agreement with other results obtained from previous studies that focus on optimizing the thermal performance of earth block walls [14,16,30,33,40].

Figure 12 presents a summary of research focused on the thermal optimization of envelope wall thicknesses for earthen constructions across various climatic contexts worldwide. Notably, in recent studies, Toure et al. [4] conducted an extensive experimental and numerical investigation to determine the time lag and decrement factor of walls made with cement-stabilized CSEB in the hot and arid climate of Senegal. Their findings align closely with those obtained in this study, showing that optimal wall thicknesses between 30 and 34 cm are sufficient to achieve good thermal comfort with a time lag of 10 to 12 hours. Similarly, Balaji et al. [14] found that the optimum thickness for homogeneous cement-stabilized earth block walls to ensure the best thermal performance lies between 25 and 40 cm. The authors concluded that these thermal performances mainly depend on the thermo-physical properties of the CSEB blocks (see Fig. 12).

Another experimental study conducted by Neya et al. [30] found that homogeneous CSEB block walls with optimal thicknesses of 22 and 35 cm stabilized with 8% cement in the hot and dry regions of Burkina Fasso have decrement factors of 0.22 and 0.23, respectively. In addition, Hall et al. [49] indicated that at the lower decrement factors values, a weak temperatures variation is obtained in the blocks CSEB walls. While, Al-Jabri et al. [50] used an experimental test program to evaluate the thermal properties of CSEB buildings in Oman. The CSEB walls provided time offsets of 1 to 7 hours and achieved lower decrement factors of 0.15 to 0.23, respectively.

Ebrahimi et al. [51] used an analytical model to optimize the design strategy of a CSEB earth block housing program in the city of Kabul. Analysis of the results suggests that the optimum thickness of a CSEB wall in the climatic context of the Kabul region is around 50 cm. Yu et al. [52] conducted an analytical study to evaluate the thermal performance of exterior envelopes of earthen buildings across five Chinese cities – Guangzhou, Kunming, Shanghai, Beijing, and Harbin. They found that a wall thickness of approximately 35.5 cm provides optimal results for homogeneous CSEB walls. Additionally, Hall et al. [43] employed the cyclic admittance method, which accounts for unsteady thermal characteristics, to study the thermal performance of earthen adobe walls. Their conclusions aligned closely with the current findings, indicating that the optimal wall thickness for acceptable thermal performance typically ranges between 30 and 40 cm.

Other authors have also investigated the impact of thermophysical properties of walls made from various materials on dynamic thermal performance. Shaik et al. [22,27] concluded that the combined effects of wall thickness and thermophysical properties significantly influence the time lag and decrement factor, which are crucial for the thermal performance of laterite material walls. Ulgen et al. [48] evaluated the effects of the thermo-physical properties of bricks-based walls on time lag and decrement factor using a Fourier analytical method. The main conclusion obtained in this work that the effect of the increase in thermal diffusivity led to the increase of the decrement factor and a decrease of time lag values.

Moreover, Jin et al. [16] found that the time lag of the heat flux increases with increasing thermal capacity and wall thickness, while it decreases with increasing thermal conductivity of the homogeneous wall. As for the heat flux decrement factor, it tends to decrease and increase with increasing thermal capacity and wall thickness.

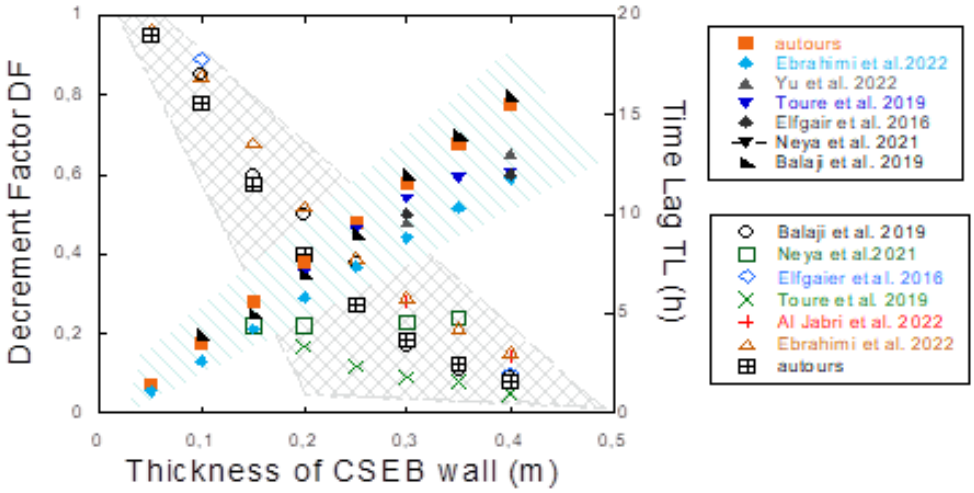

Fig. 12. Decrement factor and time lag of earthen building materials in response to varying CSEB wall thickness according to the literature

3.6. Multiple linear regression analysis

3.6.1. MLR models

The translation of the relationship generated between the dependent variables (Yi) and studied independent variables (Xj) is widely investigated by the statistical method of MLR analysis due to its large information about the correlation occurred between the predicted values using developed model and the experimental data. The statistical analysis investigated during this work using MLR analysis proposed four mathematical models as indicated below for the prediction of different dynamic thermal parameters of DF, TL, U and Y.

$$DF = 0.63 - 0.88\,X_1 + 0.58\,X_2 - 0.003\,X_3 \quad (18)$$

$$TL = 0.88 + 34.68\,X_1 - 17.08\,X_2 + 0.0018\,X_3 \quad (19)$$

$$U = 2.84 - 3.23\,X_1 + 2.69\,X_2 + 0.051\,X_3 \quad (20)$$

$$Y = 4.44 + 0.24\,X_1 + 1.02\,X_2 + 0.053\,X_3 \quad (21)$$

where X_1; X_2 and X_3 indicate the considered independent variables of blocks thicknesses, cement content and compaction pressures applied for manufacturing different studied samples, respectively. The values of different models coefficients indicate clearly that the variation of all dynamic thermal parameters mainly depend with the variation of the three considered independent variables. As a result, the values of DF decrease with increasing of

the wall thickness and the compaction pressure but the cement additions have negative effect on the DF parameter, the developed model indicates that the increasing of cement content lead to increase of DF values. In contrast, the values of TL parameter increase with increasing of wall thicknesses and compaction pressures of studied CSEB samples. For both parameters of U and Y, its values increase with high compactions pressures and cement content, but is not the same for wall thickness, the high values of this independent variable mainly lead to the low values of U parameter.

3.6.2. Model validation

The ability of the developed Multiple Linear Regression (MLR) models to predict the various dynamic thermal parameters as functions of the three independent variables is primarily assessed through the interpretation of statistical correlation (R) and determination (R^2) coefficients. Additionally, various regression parameters were calculated using the Analysis of Variance (ANOVA) test. This regression method generally identifies whether the model significantly explains the variability in the observed data; however, in some cases, it may indicate a limited capacity to accurately represent real-world observations.

The results summarized in Table 3 indicate the values of different statistical coefficients calculated using the MLR analysis, namely: coefficient of correlation (R), coefficient of determination (R^2), adjusted coefficient of determination (Adjusted R^2), the standard error of estimate, and the Durbin–Watson statistics parameter. The values of R parameter generally translate the correlation occurred between different considered independent variables. In this work, high values (> 0.5) are obtained for all studied thermal dynamic parameters which indicates the high correlation occurred between the predicted values using developed MLR models and the calculated results. Moreover, the values of R^2 can give a good information about the fraction values of the dependent variables that can be described by the adequate model. The findings indicate a value of 0.98 is obtained for R^2 for the developed TL model. This result concludes that 98% of the variation of TL values can be described by the variation of the three considered independents variables of wall thickness, cement content and compactions pressures. Moreover, the vales of 0.68, 0.79, 0.57 are obtained for R^2 of DF, U and Y thermal dynamic parameters. According to the previous studies, it appears that the value of R^2 mainly dependent by the number of the independent variables considered in the MLR model [53], this is can be explaining the low values obtained for Y parameter. The standard errors of 0.175, 0.643, 0.497 and 0.1668 are obtained for different DF, TL, U and Y models.

Table 3. Summary of the MLR analysis model obtained for different thermal dynamic parameters.

Models	R	R^2	Adjusted R^2	Standard error of the estimate	Durbin-Watson
DF	0.829	0.687	0.73	0.175	0.085
TL	0.988	0.977	0.975	0.643	1.972
U	0.891	0.793	0.785	0.497	0.572
Y	0.753	0.567	0.549	0.1668	0.486

The values of The Durbin–Watson statistic are also calculated during this work for the examination of the presence of an auto-correlation between the three independents variables investigated. According to the previous studies this statistical parameter varied from 0 to 4 with a midpoint of 2 [54-56]. As a result, the Table 4 indicate that the values of Durbin–

Watson statistic are less than 2. This main finding concludes the existence of the auto-correlation between the three considered independent variables of wall thicknesses, cement content and compaction pressures. The results indicated in Table 4 summarize the main findings obtained by the ANOVA test.

Table 4. ANOVA-test table obtained for the four developed MLR model

	Models	Sum of squares	Degrees of freedom (df))	Mean square	F	Sig.
DF	Regression	4.742	3	1.581	51.852	0.000
	Residual	2.162	71	0.030		
	Total	6.906	74			
TL	Regression	633.53	3	211.178	510.664	0.000
	Residual	14.887	36	0.414		
	Total	648.421	39			
U	Regression	67.281	3	22.427	90.898	0.000
	Residual	17.518	71	0.247		
	Total	84.799	74			
Y	Regression	2.591	3	0.864	31.035	0.000
	Residual	1.975	71	0.028		
	Total	4.566	74			

Indeed, the values of the sums of squares calculated for different thermal dynamic parameters translate the distinction of the global variance in the response calculated by the considered parameters and measurement errors [57]. The F-test was also conducted in order to examine the exclusion of null hypothesis and to explain the effect of each independent variables on the different characteristics of materials [58,59]. As a result, the calculated values of F for all thermal dynamic parameters are much higher than the value of F critical. The significant level (Sig.) supposed in this work is 5% (α) and from the results indicated in Table 5 it appears that all developed MLR models display values of Sig. lower than the fixed level ($0.000 < 0.05$). This main result concludes that the relationship between the three investigated independent variables and their interactions are statistically significant and they are the main reasons of the variation of studied thermal dynamic parameters. The main regression results obtained for each developed MLR model are given in Table 5 of appendix 2.

Figure 13 illustrates the residuals analysis as function of both independent variables affected the variation of dynamic thermal parameters of cement content and wall thicknesses. The results of this analysis indicate clearly the low range of residuals which are uniformly and symmetrically closed to zero, this is mainly due to the good significant of developed MLR model [60,61].

The correlation analysis between the predicted values from different developed MLR models and the calculated values of dynamic thermal parameters was also investigated in this study (Fig. 14). The results of this analysis show that the developed MLR model for TL and U parameters demonstrates strong correlation with high coefficient of determination of 0.98 and 0.8, respectively, which confirms the high performance of obtained model.

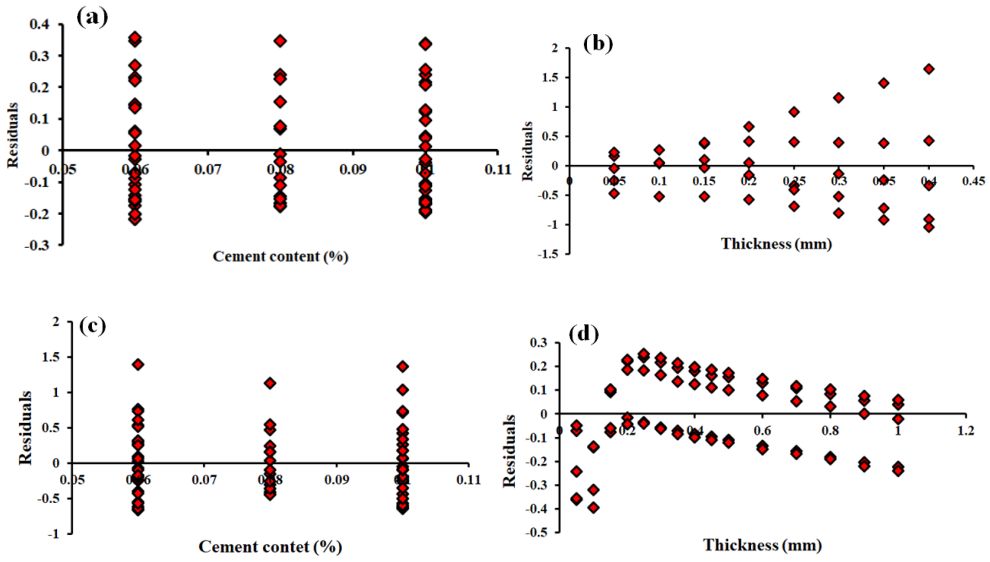

Fig. 13. Residual results as function of cement content and wall thicknesses for (a) DF, (b) TL, (c) U and (d) Y MLR models

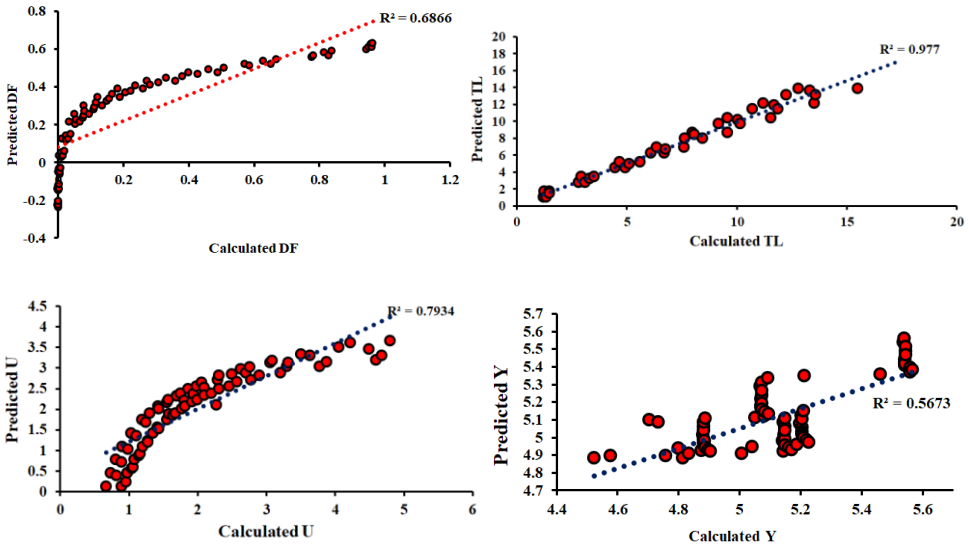

Fig. 14. Predictive values as a function of calculated results of different studied dynamic thermal parameters

In the other hand, Fig. 15 illustrates the frequency histograms of calculated values of each dynamic thermal parameter. According to the 75 tests of DF, U and Y analysis established on the CSEB samples with various manufacturing conditions, the median of 0.26, 7.48, 2.07 and 5.12 with low standard deviation of 0.31, 1.07 and 0.25 are obtained four DF, U and Y parameters. Based of 40 tests, the median of 7.48 and standard deviation of 4.08 are obtained for TL parameters.

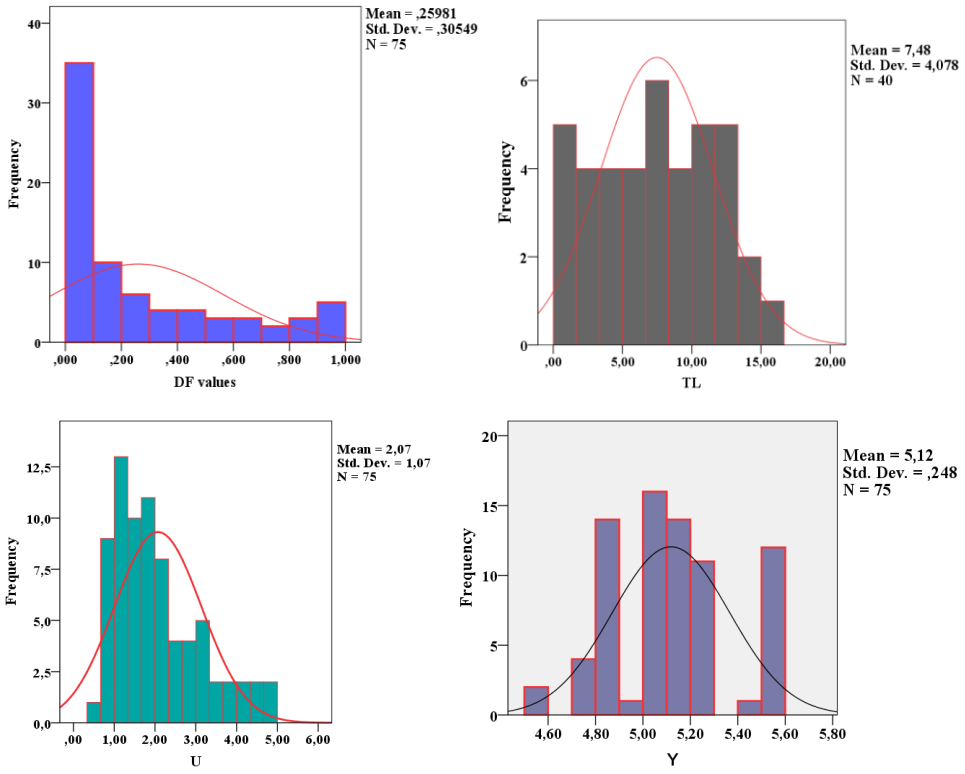

Fig. 15. Frequency histogram of different calculated studied thermal dynamic parameters

4. Conclusions

This study presents a combined analytical and experimental investigation into the dynamic thermal behavior of five types of homogeneous walls constructed with Compressed Stabilized Earth Blocks (CSEB). Based on the results obtained, the following conclusions can be drawn:

- A strong agreement was observed between the experimental results and the values of time lag and decrement factor evaluated using the admittance method.
- The intrinsic thermo-physical properties of CSEB materials and wall thickness significantly influence the dynamic thermal performance of the building envelope. Additionally, the type of sandy soil used (sourced from various sites in northern and southern Algeria) and the manufacturing method of the blocks notably affect thermal behavior.
- An increase in wall thickness leads to a decrease in decrement factor and an increase in time lag. Moreover, the surface factor and time lag are inversely related; surface factor values decrease with increasing thermal conductivity.
- Among the five types of CSEB blocks, the W2 wall configuration demonstrated the best thermal performance, with the lowest decrement factor (0.081) and the highest time lag (15.49 hours) at a thickness of 40 cm. In contrast, the W1 configuration yielded the highest decrement factor (0.168) and the lowest time lag (11.83 hours).

- Walls constructed with CSEB-2 and CSEB-5 achieve optimal thermal inertia at a reduced thickness of 30 cm. However, a greater thickness of 40 cm is necessary for CSEB-3 and CSEB-4 walls to ensure sufficient heat capacity and achieve a thermal lag between 10 and 12 hours. Considering the number of blocks required and the habitable space, W2 and W5 configurations are the most suitable for application in hot and semi-arid climates in Algeria, offering a good balance between thermal comfort and economic feasibility.
- The R^2 values indicate that the Multiple Linear Regression (MLR) model provides high accuracy in predicting the time lag (TL) and thermal transmittance (U), with values of 0.98 and 0.79, respectively. Regression analysis further revealed that cement content and wall thickness are the primary influencing factors for the decrement factor (DF) and time lag (TL), while compaction pressure plays a major role in determining the thermal transmittance (U) and thermal admittance (Y).

Perspectives for Future Research

The findings of this study open new research perspectives for the application of CSEB materials in a wider range of building types across North African climates. The thermal parameters determined here can serve as a foundation for further research and for developing future building regulations or recommendations tailored to CSEB-based construction.

Moreover, to enhance the predictive capability of thermal performance models, future studies may explore more advanced statistical and computational techniques. These include non-linear regression analysis, artificial neural networks (ANNs), and support vector machines (SVMs) – all of which could improve upon the MLR models proposed in this work.

References

[1] Briga Sá A. C. et al., "An analytical approach to assess the influence of the massive wall material, thickness and ventilation system on the Trombe wall thermal performance", *Journal of Building Physics*, 41(5), (2018), 445–468. https://doi.org/10.1177/1744259117697389

[2] Derradji L. et al., "A study on residential energy requirement and the effect of the glazing on the optimum insulation thickness", *Applied Thermal Engineering*, 112, (2017), 975–985. https://doi.org/10.1016/j.applthermaleng.2016.10.116

[3] Mokhtari F. et al., "A passive wall design to minimize building temperature swings for Algerian Saharan climate", *Science and Technology for the Built Environment*, 23(7), (2017), 1142–1150. https://doi.org/10.1080/23744731.2016.1273020

[4] Toure P. M. et al., "Experimental determination of time lag and decrement factor", *Case Studies in Construction Materials*, 11, (2019), e00298. https://doi.org/10.1016/j.cscm.2019.e00298

[5] Turco C. et al., "Optimisation of Compressed Earth Blocks (CEBs) using natural origin materials: A systematic literature review", *Construction and Building Materials*, 309, (2021), 125140. https://doi.org/10.1016/j.conbuildmat.2021.125140

[6] Mahdad M. et al., "Thermal performance evaluation of traditional buildings flat roofs in a hot and arid climate of Algeria", *Journal of Architectural and Engineering Research*, 8, (2025), 49–61. https://doi.org/10.54338/27382656-2025.8-05

[7] Labed S. et al., "Effect of tomato and pepper stem waste on thermal and physical properties of raw earth blocks", *Iranian Journal of Science and Technology, Transactions of Civil Engineering*, (2025). https://doi.org/10.1007/s40996-025-01870-x

[8] Kallou A. et al., "Performance of compressed earth blocks reinforced with natural fibers", *Budownictwo i Architektura*, 24(1), (2025), 25–49. https://doi.org/10.35784/bud-arch.6179

[9] Marletta L. et al., "Using the dynamic thermal properties to assess the internal temperature swings in free running buildings. A general model and its validation according to ISO 13792", *Energy and Buildings*, 87, (2015), 57–65. https://doi.org/10.1016/j.enbuild.2014.11.025

[10] Giuffrida G. et al., "Analysis of the thermal performances of uninsulated and bio-based insulated compressed earth blocks walls: from the material to the wall scale", *Journal of Building Engineering*, 90, (2024), 109370. https://doi.org/10.1016/J.JOBE.2024.109370

[11] Abdel Gelil Mohamed N. et al., "Structural, acoustical, and thermal evaluation of an experimental house built with reinforced/hollow interlocking compressed stabilized earth brick-masonry", *Journal of Building Engineering*, 86, (2024), 108790. https://doi.org/10.1016/J.JOBE.2024.108790

[12] Ayed R. et al., "Improving the thermal and mechanical performance of cement-based mortars for reinforcing masonry structures: computational and experimental methods", *Energy Efficiency*, 17, no. 7, (2024), p. 80. https://doi.org/10.1007/s12053-024-10263-4

[13] Nematchoua M. K. et al., "Study of the economical and optimum thermal insulation thickness for buildings in a wet and hot tropical climate: Case of Cameroon", *Renewable and Sustainable Energy Reviews*, 50, (2015), 1192–1202. https://doi.org/10.1016/j.rser.2015.05.066

[14] Balaji N. C. et al., "Dynamic thermal performance of conventional and alternative building wall envelopes", *Journal of Building Engineering*, 21, (2019), 373–395. https://doi.org/10.1016/j.jobe.2018.11.002

[15] Ding Y. et al., "Optimization approach of passive cool skin technology application for the Building's exterior walls", *Journal of Cleaner Production*, 256, (2020), 120751. https://doi.org/10.1016/j.jclepro.2020.120751

[16] Jin X. et al., "Thermal performance evaluation of the wall using heat flux time lag and decrement factor", *Energy and Buildings*, 47, (2012), 369–374. https://doi.org/10.1016/j.enbuild.2011.12.010

[17] Daouas N., "A study on optimum insulation thickness in walls and energy savings in Tunisian buildings based on analytical calculation of cooling and heating transmission loads", *Applied Energy*, 88(1), (2011), 156–164. https://doi.org/10.1016/j.apenergy.2010.07.030

[18] Yumrutaş R. et al., "Periodic solution of transient heat flow through multilayer walls and flat roofs by complex finite Fourier transform technique", *Building and Environment*, 40(8), (2005), 1117–1125. https://doi.org/10.1016/j.buildenv.2004.09.005

[19] Zedan M. F. and Mujahid A. M., "An efficient solution for heat transfer in composite walls with periodic ambient temperature and solar radiation", *International Journal of Ambient Energy*, 14(2), (1993), 83–98. https://doi.org/10.1080/01430750.1993.9675599

[20] Granja A. D. and Labaki L. C., "Influence of external surface colour on the periodic heat flow through a flat solid roof with variable thermal resistance", *International Journal of Energy Research*, 27(8), (2003), 771–779. https://doi.org/10.1002/er.915

[21] Lu X. et al., "Transient analytical solution to heat conduction in composite circular cylinder", *International Journal of Heat and Mass Transfer*, 49(1–2), (2006), 341–348. https://doi.org/10.1016/j.ijheatmasstransfer.2005.06.019

[22] Shaik S. and Talanki A. B. P. S., "Optimizing the position of insulating materials in flat roofs exposed to sunshine to gain minimum heat into buildings under periodic heat transfer conditions", *Environmental Science and Pollution Research*, 23(10), (2015), 9334–9344. https://doi.org/10.1007/s11356-015-5316-7

[23] Zedan M. F. and Mujahid A. M., "Laplace transform solution for heat transfer in composite walls with periodic boundary conditions", *Journal of Heat Transfer (Transactions of the ASME (American Society of Mechanical Engineers), Series C);(United States)*, 115(1), (1993), 263–265. https://doi.org/10.1115/1.2910659

[24] Najim K. B., "External load-bearing walls configuration of residential buildings in Iraq and their thermal performance and dynamic thermal behaviour", *Energy and Buildings*, 84, (2014), 169–181. https://doi.org/10.1016/j.enbuild.2014.07.064

[25] Evola G. and Marletta L., "A dynamic parameter to describe the thermal response of buildings to radiant heat gains", *Energy and Buildings*, 65, (2013), 448–457. https://doi.org/10.1016/j.enbuild.2013.06.026

[26] Yuan J., "Impact of insulation type and thickness on the dynamic thermal characteristics of an external wall structure", *Sustainability*, 10(8), (2018), 2835. https://doi.org/10.3390/su10082835

[27] Shaik S. and Setty A. B. T. P., "Influence of ambient air relative humidity and temperature on thermal properties and unsteady thermal response characteristics of laterite wall houses", *Building and Environment*, 99, (2016), 170–183. https://doi.org/10.1016/j.buildenv.2016.01.030

[28] Kalinović S. M. and Djoković J. M., "Analysis of dynamic thermal performance of the walls in residential buildings in Serbia", *Proceedings of the Institution of Mechanical Engineers, Part C: Journal of Mechanical Engineering Science*, 235(20), (2021), 4851–4861. https://doi.org/10.1177/0954406220941894

[29] El Fgaier F. et al., "Dynamic thermal performance of three types of unfired earth bricks", *Applied Thermal Engineering*, 93, (2016), 377–383. https://doi.org/10.1016/j.applthermaleng.2015.09.009

[30] Neya I. et al., "Impact of insulation and wall thickness in compressed earth buildings in hot and dry tropical regions", *Journal of Building Engineering*, 33, (2021), 101612. https://doi.org/10.1016/j.jobe.2020.101612

[31] Mansour M. and Hachicha M., "The vulnerability of Tunisian agriculture to climate change", *Emerging Technologies and Management of Crop Stress Tolerance*, 2, (2014), 485–500. https://doi.org/10.1016/B978-0-12-800875-1.00021-1

[32] Benidir A. et al., "Earth construction durability: in-service deterioration of Compressed and Stabilized Earth Block (CSEB) housing in Algeria", in XV International Conference on Durability of Building Materials and Components (DBMC 2020), 2020.

[33] Mahdad M. et al., "Experimental assessment of mechanical behavior of a compressed stabilized earth blocks (CSEB) and walls", *Journal of Materials and Engineering Structures «JMES»*, 8(1), (2021), 95–110.

[34] Benouali H. et al., "Monitoring des constructions en terre en Algérie. Phase de recherche.", 2010.

[35] Mahdad M. and Benidir A., "Hydro-mechanical properties and durability of earth blocks: Influence of different stabilisers and compaction levels", *International Journal of Sustainable Building Technology and Urban Development*, 9(2), (2018), 44-60,. https://doi.org/10.22712/susb.20180006

[36] Mahdad M. et al., "Etude analytique en régime dynamique des performances thermiques des parois en blocs de terre stabilisée", *Academic Journal of Civil Engineering*, 40(2), (2023), 1–9. https://doi.org/10.26168/ajce.40.2.37

[37] EN 993–15, "EN 993–15, Methods of test for dense shaped refractory products – Determination of thermal conductivity by the hot-wire (parallel) method.", *European Committee for Standardization*, 2005.

[38] ASTM C518-21: Standard Test Method for Steady-State Thermal Transmission Properties by Means of the Heat Flow Meter Apparatus, 2021. https://doi.org/10.1520/C0518-21

[39] ISO 12571: Hygrothermal performance of building materials and products-Determination of hygroscopic sorption properties, 2021.

[40] ISO 13786, Thermal performance of building components — Dynamic thermal characteristics — Calculation methods, 2009.

[41] Wang L. and Aslani F., "Electrical resistivity and piezoresistivity of cement mortar containing ground granulated blast furnace slag", *Construction and Building Materials*, 263, (2020), 120243. https://doi.org/10.1016/j.conbuildmat.2020.120243

[42] Yumrutaş R. et al., "Estimation of total equivalent temperature difference values for multilayer walls and flat roofs by using periodic solution", *Building and Environment*, 42(5), (2007), 1878–1885. Estimation of total equivalent temperature difference values for multilayer walls and flat roofs by using periodic solution

[43] Hall M. and Allinson D., "Assessing the moisture-content-dependent parameters of stabilised earth materials using the cyclic-response admittance method", *Energy and Buildings*, 40(11), (2008), 2044–2051. https://doi.org/10.1016/j.enbuild.2008.05.009

[44] Balaji N. C. et al., "Dynamic thermal performance of conventional and alternative building wall envelopes", *Journal of Building Engineering*, 21, (2019), 373–395. https://doi.org/10.1016/j.jobe.2018.11.002

[45] Shaik S. and Setty A. B. T. P., "Influence of ambient air relative humidity and temperature on thermal properties and unsteady thermal response characteristics of laterite wall houses", *Building and Environment*, 99, (2016), 170–183. https://doi.org/10.1016/j.buildenv.2016.01.030

[46] Asan H., "Numerical computation of time lags and decrement factors for different building materials", *Building and Environment*, 41(5), (2006), 615–620. https://doi.org/10.1016/j.buildenv.2005.02.020

[47] Moschella A. et al., "A methodology for an integrated approach for seismic and energy refurbishment of historic buildings in mediterranean area", *Sustainability*, 10(7), (2018), 2448. https://doi.org/10.3390/su10072448

[48] Ulgen K., "Experimental and theoretical investigation of effects of wall's thermophysical properties on time lag and decrement factor", *Energy and Buildings*, 34(3), (2002), 273–278. https://doi.org/10.1016/S0378-7788(01)00087-1

[49] Hall M. R. et al., *Modern earth buildings: Materials, engineering, constructions and applications*. Elsevier, 2012.

[50] Al-Jabri K. et al., "Structural and thermal performance of sustainable interlocking compressed earth blocks masonry units made with produced water from oilfields", *Case Studies in Construction Materials*, 17, (2022), e01186. https://doi.org/10.1016/j.cscm.2022.e01186

[51] Ebrahimi M. H. et al., "Sustainable construction for affordable housing program in Kabul", *Journal of Contemporary Urban Affairs*, 6(1), (2022), 23–35.

[52] Yu S. et al., "Research on optimization of the thermal performance of composite rammed earth construction", *Energies*, 15(4), (2022), 1519. https://doi.org/10.3390/en15041519

[53] Silva A. et al., *Methodologies for service life prediction of buildings: with a focus on façade claddings*, Green Ener ed. The registered company is Springer International Publishing AG Switzerland, 2016.

[54] Unamba U. K. et al., "Predictive model of the compressive strength of concrete containing coconut shell ash as partial replacement of cement using multiple regression analysis", 2021.

[55] Wu S. S. et al., "Predictive modeling of high-performance concrete with regression analysis", in 2010 IEEE International Conference on Industrial Engineering and Engineering Management, 2010, 1009–1013.

[56] Keleştemur O. et al., "Statistical analysis for freeze-thaw resistance of cement mortars containing marble dust and glass fiber", *Materials and Design*, 60, (2014), 548–555. https://doi.org/10.1016/j.matdes.2014.04.013

[57] Abellan-Garcia J. et al., "ANOVA-guided assessment of waste glass and limestone powder influence on ultra-high-performance concrete properties", *Case Studies in Construction Materials*, 20, (2024), e03231. https://doi.org/10.1016/j.cscm.2024.e03231

[58] Fakhri M. and Amoosoltani E., "The effect of Reclaimed Asphalt Pavement and crumb rubber on mechanical properties of Roller Compacted Concrete Pavement", *Construction and Building Materials*, 137, (2017), 470–484. https://doi.org/10.1016/j.conbuildmat.2017.01.136

[59] Montgomery D. C. et al., *Introduction to linear regression analysis*. John Wiley & Sons, 2021.

[60] Singh P. et al., "Development of performance-based models for green concrete using multiple linear regression and artificial neural network", *International Journal on Interactive Design and Manufacturing (IJIDeM)*, 18(5), (2024), 2945–2956. https://doi.org/10.1007/s12008-023-01386-6

[61] Chai C. et al., "Statistical modelling of the service life prediction of painted surfaces", *International Journal of Strategic Property Management*, 19(2), (2015), 173–185. https://doi.org/10.3846/1648715X.2015.1031853

[62] Davies M. G., "The thermal response of an enclosure to periodic excitation: the CIBSE approach", *Building and Environment*, 29, no. 2, (1994), 217–235.

Appendix 1: The cyclic-response admittance method

The admittance method is used in this study in order to calculate unsteady state thermal response parameters values using matrices. This method generally used to simplify the temperature and energy cycles for a fabric element that is subjected to sinusoidal temperature variations at the sol-air environmental node [28].

This analysis focuses on one-dimensional transient thermal conduction through a wall with initial condition and two time-dependent boundary conditions.

$$\rho C_p \frac{\partial T(x,t)}{\partial t} = \lambda \frac{\partial^2 T(x,t)}{\partial x^2} \qquad 0 < x < L,\ t > 0 \tag{1}$$

λ, ρ et C_p are thermal conductivity, density and specific heat respectively.

The boundary conditions associated with equation (1) are:

$$-\lambda \frac{\partial T}{\partial x}(0,t) = h_i[T(0,t) - T_i] \ \text{ for } \ x = 0, t > 0 \tag{2}$$

$$-\lambda \frac{\partial T}{\partial x}(L,t) = h_0[T_o(t) - T(L,t)] \ \text{ for } \ x = L, t > 0 \tag{3}$$

The initial condition is given as follows:

$$T(x,0) = T_0 \ \text{ at } t = 0,\ 0 \le x \le L \tag{4}$$

where: (h_i, T_i) and (h_0, T_0) are respectively the heat transfer coefficients and the temperatures taking into account the convective and radiative effects respectively on the internal and external surfaces of the wall [14].

Space and time-independent solution is used for the resolution of equation (1) with boundary and initial conditions (2), (3) and (4). It allows to describe the dependence in the imaginary domain of temperatures and thermal flows on both sides of an opaque wall. The solution is sought in the following form, [62]:

$$T(x,t) = A.\exp\left(x/\xi\right)\exp\left(t/\zeta\right) \tag{5}$$

where, ξ and ζ have units of distance and time respectively.

By introducing the form (5) into the heat equation (1), we obtain the relation: $\xi^2 = \alpha\zeta$. Where α is the thermal diffusivity of the wall. For a wall subjected to periodic excitation of period P, we obtain a periodic solution for the temperature taking into account the relationship:

$$\xi^2 = \frac{\alpha P}{2j\pi} \ \text{ where } \ j^2 = -1 \tag{6}$$

Thus, it can be obtained a periodic solution with period P.

$$\frac{x}{\xi} = \frac{x}{\pm\left(\alpha P/_{j2\pi}\right)^{1/2}} = \pm(i+j)\left(\frac{\pi\rho C_p x^2}{\lambda P}\right)^{1/2} \tag{7}$$

In this case, the matrix relationship between flux and internal and external temperatures is given in equation 8.

$$\begin{bmatrix} T_{pi} \\ q_{pi} \end{bmatrix} = \begin{bmatrix} E_{11} & E_{12} \\ E_{21} & E_{22} \end{bmatrix} \begin{bmatrix} T_{pO} \\ q_{pO} \end{bmatrix} \tag{8}$$

The transfer matrix is defined below:

$$\begin{bmatrix} E_{11} & E_{12} \\ E_{21} & E_{22} \end{bmatrix} = \begin{bmatrix} 1 & -R_i \\ 0 & 1 \end{bmatrix} \begin{bmatrix} (A_1 + jA_2) & (A_3 + jA_3)/a \\ a(-A_4 + jA_3) & (A_1 + jA_2) \end{bmatrix} \begin{bmatrix} 1 & -R_0 \\ 0 & 1 \end{bmatrix} \tag{9}$$

T_{pi}, q_{pi}, T_{pO} et q_{pO} are respectively temperature and heat flux at both internal and external surfaces. R_i and R_O represent the inside and outside film resistances, respectively.

Two parameters appear in the definition of the transmission matrix, namely the cyclic thickness z and the characteristic of admittance slab a, defined in Eqs. (10) and (11) :

$$z = \sqrt{\frac{\pi L^2}{\alpha \mathrm{P}}} = \sqrt{\frac{\omega L^2}{2\alpha}} \tag{10}$$

$$a = \sqrt{j\omega\lambda\rho C_p} \tag{11}$$

Thermal transmittance U is calculated as the following equation:

$$U = \frac{1}{R_i + R_c + R_O} \tag{12}$$

where: $R_c = \frac{\mathrm{L}}{\lambda}$

The thermal admittance (Y) is calculated as indicated in the following equation:

$$Y_c = -\frac{E_{22}}{E_{12}},\ Y = |Y_c| \tag{13}$$

The decrement factor f presents the DF, is the amplitude of thermal admittance Y, normalized with respect to the steady thermal transmittance U, calculated using the relationship:

$$f_h = \frac{Y_{12}}{U} = -\frac{1}{UE_{12}};\ f = |f_h| \tag{14}$$

Φ presents the TL obtained between the timing of the peak inside temperature and the peak heat transfer out of the outer surface.

$$\phi = \frac{12}{\pi} arctan\left(\frac{Im(f_c)}{Re(f_c)}\right) = \frac{12}{\pi} arctan\left(\frac{Im\left(-\frac{1}{UE_{12}}\right)}{Re\left(-\frac{1}{UE_{12}}\right)}\right) \quad (15)$$

The surface factor Fis calculated as follows.

$$\left|F = 1 - R_{int}\frac{E_{11}}{E_{22}}\right| \quad (16)$$

Appendix 2: Statistical parameters of MLR analysis

Table 5. The values of the regression coefficients of thermal dynamics parameters

		Non-standardized coefficients		Standardized coefficients	Statistical t	Sig.	Collinearity	
		B	Standard error	Beta			Tolerance	VIF
DF	Constant	0.633	0.106	/	5.971	0.000	/	/
	Thickness	-0.879	0.071	-0.828	-12.459	0.000	1.000	1.000
	Cement content	0.584	1.154	0.034	0.506	0.000	0.954	1.048
	Compaction pressures	-0.003	0.007	0.027	0.393	0.695	0.954	1.048
TL	Constant	0.883	0.553	/	1.596	0.119	/	/
	Thickness	34.675	0.888	0.986	39.023	0.000	0.999	1.001
	Cement content	-17.08	5.786	-0.076	-2.953	0.006	0.965	1.036
	Compaction pressures	0.018	0.033	0.014	0.549	0.587	0.964	1.038
U	Constant	2.840	0.306	/	9.287	0.000	/	/
	Thickness	-3.231	0.201	-0.868	-16.075	0.000	0.998	1.002
	Cement content	2.687	3.265	0.045	0.823	0.413	0.965	1.037
	Compaction pressures	0.051	0.018	0.153	2.779	0.007	0.963	1.039
Y	Constant	4.435	0.101	/	43.821	0.000	/	/
	Thickness	0.237	0.067	0.275	3.522	0.001	1.000	1.000
	Cement content	1.015	1.102	0.074	0.921	0.360	0.954	1.048
	Compaction pressures	0.054	0.006	0.682	8.530	0.000	0.954	1.048